

**Figure 1** Rpt3-Thr25 phosphorylation drives G1 and S phase of the cell cycle. The image on the left shows the structure of the top half of the proteasome, with  $\beta$  subunits in blue,  $\alpha$  subunits in green and ATPase subunits in cyan — except for Rpt3, which is in red. DYRK2 phosphorylates Rpt3 at Thr25 (presumed location indicated with yellow star). Thr25 phosphorylation activates the 26S proteasome and drives the cell cycle through G1/S, probably through enhanced degradation of cell cycle inhibitors such as p21 and p27. Figure adapted from ref. 3, Nature Publishing Group.

degradation is not thought to be ubiquitin dependent, indicating that Rpt3-Thr25 phosphorylation by DYRK2 very broadly regulates protein flux through the proteasome. Like mutation of the Thr25 phosphorylation site, CRISPR/Cas9-mediated knockout of DYRK2 negatively affected cellular proliferation in cell lines. Consistent with this finding, tumour xenografts in mice grew significantly slower when DYRK2 was knocked out, and in human breast cancer patients, high levels of DYRK2 mRNA have been previously correlated with poorer prognosis. Importantly, DYRK2 knockout sensitized a breast-cancer-derived cell line to proteasome inhibition by

Velcade (bortezomib). The importance of Rpt3-Thr25 phosphorylation in cells suggests that simultaneous targeting of the proteasome by interfering with DYRK2 function and the proteasome active sites (using Velcade) could yield synergetic therapeutic effects that could expand the utility of proteasome inhibitors to a broader range of tumour types. Additionally, several neurodegenerative diseases are associated with the accumulation of toxic proteins that the proteasome fails to degrade. Small molecules that inhibit protein deubiquitination are promising tools for stimulating the clearing of the toxic proteins<sup>14</sup>, and it is likewise possible that boosting proteasome activity through

enhanced DYRK2-dependent phosphorylation might counter proteotoxic stress, as has recently been proposed for phosphorylation of the proteasome subunit Rpn6 (ref 15).

The regulatory function of Rpt3-Thr25 phosphorylation uncovered in the study by Guo *et al.*, combined with prior characterization of Rpt6 phosphorylation in neurons<sup>6</sup> and the fact that there are hundreds of other documented post-translational modification events on the proteasome<sup>8</sup>, suggests that we may be on the verge of breakthroughs in the understanding of proteasome function and regulation. A mechanistic understanding of these events promises to lead to a vastly expanded repertoire of therapeutics aimed at proteasome-associated activities for the treatment of cancers and also, possibly, neurodegenerative diseases.

#### COMPETING FINANCIAL INTERESTS

The authors declare no competing financial interests.

1. Craney, A. & Rape, M. *Curr. Opin. Cell Biol.* **25**, 704–710 (2013).
2. Dick, L. R. & Fleming, P. E. *Drug Discov. Today* **15**, 243–249 (2010).
3. Guo, X. *et al. Nat. Cell Biol.* **18**, 202–212 (2016).
4. Bence, N. F., Sampat, R. M. & Kopito, R. R. *Science* **292**, 1552–1555 (2001).
5. Ye, J. *eLife* **3**, e02062 (2014).
6. Djakovic, S. N., Schwarz, L. A., Barylko, B., DeMartino, G. N. & Patrick, G. N. *J. Biol. Chem.* **284**, 26655–26665 (2009).
7. Zhang, F. *et al. Cell* **115**, 715–725 (2003).
8. Hirano, H., Kimura, Y. & Kimura, A. *J. Proteom.* <http://dx.doi.org/10.1016/j.jprot.2015.11.016> (2015).
9. Peth, A., Uchiki, T. & Goldberg, A. L. *Mol. Cell* **40**, 671–681 (2010).
10. Bech-Otschir, D. *et al. Nat. Struct. Mol. Biol.* **16**, 219–225 (2009).
11. Satoh, K., Sasajima, H., Nyomura, K. I., Yokosawa, H. & Sawada, H. *Biochemistry* **40**, 314–319 (2001).
12. Finley, D., Chen, X. & Walters, K. J. *Trends Biochem. Sci.* **41**, 77–93 (2015).
13. Yao, T. *Nat. Struct. Mol. Biol.* **22**, 652–653 (2015).
14. Lee, B.-H. *et al. Nature* **467**, 179–184 (2010).
15. Lokireddy, S., Kukushkin, N. V. & Goldberg, A. L. *Proc. Natl Acad. Sci. USA* **112**, E7176–E7185 (2015).

## Actin puts the squeeze on *Drosophila* glue secretion

Christien J. Merrifield

**An actin filament coat promotes cargo expulsion from large exocytosing vesicles, but the mechanisms of coat formation and force generation have been poorly characterized. Elegant imaging studies of the *Drosophila melanogaster* salivary gland now reveal how actin and myosin are recruited, and show that myosin II forms a contractile ‘cage’ that facilitates exocytosis.**

Christien J. Merrifield is at the Laboratoire d’Enzymologie et Biochimie Structurales, CNRS Division of Cell Biology, Avenue de la Terrasse, Gif-sur-Yvette 91198, France.  
e-mail: [christien.merrifield@2bc.paris-saclay.fr](mailto:christien.merrifield@2bc.paris-saclay.fr)

In the process of exocytosis, secretory vesicles fuse with the plasma membrane and release their cargo to the cell exterior. The core mechanism of SNARE-mediated membrane fusion

and the formation of a fusion pore is well conserved, even though secretory vesicles come in a remarkably wide range of sizes containing a range of different cargos<sup>1,2</sup>. However, events

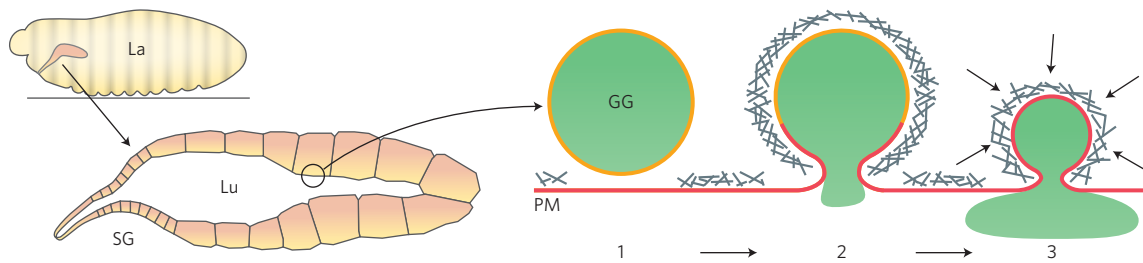


**Figure 1** Exocytosis of glue granules in the *Drosophila* salivary gland. The *Drosophila* larva (La) has a pair of tube-like salivary glands (SG), which empty into a common duct that opens into the larval pharynx. In this profile diagram of a larva, only one salivary gland is visible. Before expectoration, glue granules (GG) exocytose glue (green) into the salivary gland lumen (Lu). Glue granule exocytosis proceeds as follows. (1) Intracellular  $\text{Ca}^{2+}$  rises, cortical actin clears, the glue granule docks and fuses with the plasma membrane via  $\text{Ca}^{2+}$ -dependent exocytosis. (2) Mixing between the granule membrane (orange) and plasma membrane (PM, red) triggers F-actin polymerization (grey) through the sequential recruitment of Dia, WASp and Arp2/3 (not shown). An F-actin shell grows from the site of fusion over the surface of the vesicle and thickens. (3) Simultaneous myosin II recruitment (not shown, steps 2–3) causes the actomyosin meshwork to contract, ‘scrunching’ the granule and squeezing the glue into the salivary gland lumen. Following vesicle collapse, the actomyosin machinery disassembles (not shown).

immediately following fusion pore formation in the ‘fusion pore expansion’ phase may vary<sup>3</sup>. Thus, when a ~50 nm synaptic vesicle full of soluble neurotransmitter fuses with the plasma membrane — and given the fusion pore is allowed to expand freely — the vesicle will readily collapse due to membrane tension and release its soluble cargo by diffusion<sup>4</sup>. By contrast, when a ~1–2  $\mu\text{m}$  vesicle full of viscous or semi-solid cargo (such as lung surfactant or von Willebrand factor) fuses with the plasma membrane, the cargo resists vesicle collapse and without further mechanical assistance the vesicle remains frozen or collapses only very slowly<sup>5–7</sup>. Furthermore, in the case of giant granules exocytosing into the lumen of a secretory gland, a positive hydrostatic pressure in the lumen also counters vesicle collapse and cargo extrusion.

An established body of literature has shown that cells tackle the big granule/viscous cargo problem using a compressive actin coat to ‘scrunch’ vesicles into the plasma membrane and actively extrude cargo<sup>6–8</sup>. The first observations that actin and myosin are involved in exocytosis of large vesicles were made several decades ago using immunoelectron microscopy<sup>7</sup>. In a perceptive study, Segawa and Yamashina<sup>7</sup> hypothesized that cortical actin may initially act as a barrier that must clear to allow fusion, and that later the actomyosin coat seen on fusing vesicles may provide a compressive force to facilitate vesicle collapse. More recent studies used live-cell imaging to show that the exocytosis of Weibel–Palade bodies or surfactant in lung alveolar cells did indeed require a combination of actin polymerization, myosin II recruitment and compression of the resulting actomyosin coat to drive granule collapse and cargo expulsion<sup>6,7</sup>.

However, in these later studies, exocytic events were imaged *en face* and some details of the mechanism were inferred rather than measured directly. Now, in two elegant time-resolved 3D imaging studies from the Shilo<sup>8</sup> and Ten Hagen<sup>9</sup> labs, the molecular mechanism of the actin coat formation and actomyosin-dependent vesicle compression has been imaged in unprecedented detail at the level of single exocytic events in the *Drosophila* salivary gland.

The *Drosophila* salivary glands play an essential role as a ‘glue gun’ in the larva, expectorating viscous glue through the larval mouth that is used to stick the nascent puparium to a solid substrate<sup>10</sup> (Fig. 1). The glue is initially stored in glue granules — vesicles of 3–7  $\mu\text{m}$  diameter, which pack the cells lining the salivary gland wall — and in the 4–5 hours before expectoration, a pulse of ecdysone triggers  $\text{Ca}^{2+}$ -dependent glue granule exocytosis into the salivary gland lumen, which becomes engorged with glue<sup>11</sup>. By carefully teasing out the larval salivary glands and triggering glue granule exocytosis *ex vivo* with a pulse of ecdysone, the researchers could then use confocal microscopy to image individual granule exocytic events with unprecedented clarity.

The sequence of events comprising glue granule exocytosis and glue extrusion may now be briefly summarized as follows. First, cortical actin was dynamically cleared from the nascent site of glue granule fusion<sup>9</sup>, consistent with an old hypothesis that actin may normally act as a barrier to exocytosis<sup>7,12</sup>. Using the accessibility of fluorescent dextran as a temporospatial marker of granule fusion, it was discovered that actin began to polymerize over the secretory granule from the site of fusion<sup>8,9</sup>. This suggested that lipids in the plasma membrane — most

probably phosphoinositide(s) — diffused into the vesicle membrane after exocytosis and triggered actin polymerization as the membrane identity switched from ‘granule’ to ‘plasma membrane’. Indeed, PIP<sub>2</sub>, which is present in the plasma membrane, was only detected at the vesicle surface after fusion<sup>8,9</sup>. Surprisingly, F-actin was detected at the vesicle surface before the recruitment of Arp2/3 components<sup>8,9</sup>, consistent with the formation of linear actin through a mechanism involving the formin Dia<sup>8</sup>. Components of the Arp2/3 complex were subsequently recruited as a branched F-actin shell formed around the fusing vesicle<sup>8,9</sup>. Following actin polymerization, the timing of RhoI/Rok-dependent recruitment of myosin II strongly suggested that actomyosin contraction may have delivered the compressive ‘*coup de grace*’ that drove vesicle collapse<sup>8,9</sup>. Myosin II distribution initially seemed to be relatively uniform over the vesicle, but rapidly reorganized into stripes perpendicular to the apical membrane and spanning the vesicle surface, most probably through a mechanism of self-organization<sup>8</sup>.

The observations presented were clearly suggestive, but did actin polymerization and the actomyosin meshwork actually do anything useful? Treatment with latrunculin or cytochalasin D blocked vesicle collapse and caused vesicles to fuse with one another, suggesting that early actin recruitment to the granule surface acted as a barrier that prevented compound fusion<sup>9</sup>. Furthermore, the two studies showed that knockdown of the actin nucleation promotion factor WASp<sup>9</sup> and the Arp2/3 complex<sup>8,9</sup> blocked vesicle collapse, and instead fused vesicles became very large and sometimes separated from the plasma membrane<sup>9</sup>. Moreover,

following Arp2/3 knockdown, the properties of the actin shell were disrupted and myosin II distribution became uniform, hinting that the degree of F-actin branching and perhaps the density of the F-actin shell was essential for efficient vesicle contraction<sup>8</sup>. Collectively these results clearly show that the ordered polymerization of actin and contraction of the branched actomyosin shell are required for individual vesicles to fuse with the plasma membrane and properly collapse.

As well as providing detailed insight into the vesicle collapse mechanism, these two studies raise many new questions. For instance, the global mechanics of the system remain undefined and it is not known how much of the pressure required for glue expectoration comes from the development of intrinsic luminal pressure through membrane trafficking and how much comes from muscular contraction of the adhering larva. There are also potential — and intriguing — molecular links between glue granule exocytosis and the fate of spent *Drosophila* salivary glands that might warrant closer attention. Programmed cell death of the salivary gland rapidly follows expectoration and requires the abundant

myosin II binding protein p127<sup>13</sup>. However, whether p127 participates in glue granule exocytosis, and perhaps links exocytosis to apoptosis, remains unknown. Finally, there are curious parallels between actomyosin-mediated membrane collapse in exocytosis and actin-dependent mechanisms of endocytosis. In both cases, actin polymerization is understood to deliver a compressive force to a spheroidal membrane bud attached to the plasma membrane by a membrane umbilicus; yet in one case this leads to vesicle collapse of an exocytic vesicle, and in the other it leads to membrane scission and the liberation of an endocytic vesicle. How the cell maintains the identity of the highly curved membrane umbilicus formed during membrane fusion or fission is not entirely clear — and, indeed, there is some overlap in the set of proteins recruited. For instance, the large GTPase dynamin is essential for scission of the membrane umbilicus in endocytosis<sup>14</sup>, but is also recruited to the membrane umbilicus formed at sites of exocytosis where it can control fusion pore expansion<sup>15</sup>. The experimental system described here<sup>8,9</sup> seems an excellent vehicle to investigate the molecular overlap between the exocytic and

endocytic machineries, especially with regards to phosphoinositide metabolism and the control of actin polymerization. Overall it remains clear that the combination of *Drosophila* genetics and live-cell imaging will be a powerful model system to further dissect the exocytosis of viscous cargo from large exocytic vesicles.

#### COMPETING FINANCIAL INTERESTS

The author declares no competing financial interests.

1. Jahn, R. & Fasshauer, D. *Nature* **490**, 201–207 (2012).
2. Burkhardt, P. *J. Exp. Biol.* **218**, 506–514 (2015).
3. Neuland, K. & Frick, M. *Commun. Integr. Biol.* **8**, e1018496 (2015).
4. Kozlov, M. M. & Chernomordik, L. V. *Curr. Opin. Struct. Biol.* **33**, 61–67 (2015).
5. Miklavc, P. *et al. J. Cell Sci.* **125**, 2765–2774 (2012).
6. Nightingale, T. D. *et al. J. Cell Biol.* **194**, 613–629 (2011).
7. Segawa, A. & Yamashina, S. *Cell Struct. Funct.* **14**, 531–544 (1989).
8. Rouso, T., Schejter, E. D. & Shilo, B.-Z. *Nat. Cell Biol.* **18**, 181–190 (2016).
9. Tran, D. T., Masedunskas, A., Weigert, R. & Ten Hagen, K. G. *Nat. Commun.* **6**, 10098 (2015).
10. Fraenkel, G. & Brookes, V. J. *J. Biol. Bull.* **105**, 442–449 (1953).
11. Biyasheva, A., Do, T. V., Lu, Y., Vaskova, M. & Andres, A. *J. Dev. Biol.* **231**, 234–251 (2001).
12. Orci, L., Gabbay, K. H. & Malaisse, W. J. *Science* **175**, 1128–1130 (1972).
13. Farkas, R. *et al. Nucleus* **2**, 489–499 (2011).
14. Sundborger, A. C. & Hinshaw, J. E. *F1000Prime Rep.* **6**, 85 (2014).
15. Anantharam, A. *et al. Mol. Biol. Cell* **22**, 1907–1918 (2011).